Activity-Based Approach for Selective Molecular CO$_2$ Sensing.

Ori Green,[1‡] Patrick Finkelstein,[1‡] Miguel A. Rivero-Crespo,[1] Marius D. R. Lutz,[1] Michael K. Bogdos,[1] Michael Burger,[2] Jean-Christophe Leroux[2] and Bill Morandi[1*†]

[1] Laboratory of Organic Chemistry, Department of Chemistry and Applied Biosciences, ETH Zürich, Vladimir-Prelog-Weg 3, HCI, 8093 Zürich, Switzerland

[2] Institute of Pharmaceutical Sciences, Department of Chemistry and Applied Biosciences, ETH Zürich, Vladimir-Prelog-Weg 3, HCI, 8093 Zürich, Switzerland

ABSTRACT: Carbon dioxide (CO$_2$) impacts every aspect of life and numerous sensing technologies have been established to detect and monitor this ubiquitous molecule. However, its selective sensing at the molecular level remains an unmet challenge, despite the tremendous potential of such an approach for understanding this molecule's role in complex environments. In this work, we introduce a unique class of selective fluorescent carbon dioxide molecular sensors (CarboSen) that addresses these existing challenges through an activity-based approach. Besides the design, synthesis and evaluation of these small molecules as CO$_2$-sensors, we demonstrate their utility by tailoring their reactivity and optical properties, allowing their use in a broad spectrum of multidisciplinary applications, including atmospheric sensing, chemical reaction monitoring, enzymology, and live-cell imaging. Collectively, these results showcase the potential of CarboSen sensors as broadly applicable tools to monitor and visualize carbon dioxide across multiple disciplines.

INTRODUCTION

Carbon dioxide (CO$_2$) is a ubiquitous molecule with undeniable relevance to climate research,[1,2] biology,[3,4] ecology,[5] chemistry,[6–8] agriculture,[9] food,[10,11] and healthcare.[12,13] Detection and monitoring of CO$_2$ thus play an indispensable role in investigating and understanding the multiple facets of this molecule. Currently, a vast array of modalities and materials are available to detect and monitor CO$_2$, including nondispersive infrared sensors,[14] positron emission tomography imaging,[15] Severinghaus electrodes,[16] paper-based sensors,[17,18] hydrogels,[19,20] polymers,[21,22] frameworks,[23,24] and others.[25–27] However, despite their diversity and efficiency, these methods do not allow for selective molecular CO$_2$ sensing in complex environments,[28] such as living cells, hindering research efforts and applications across multiple areas.[3]

Activity-Based Sensing (ABS), a term coined by Chang and coworkers, has proven extremely powerful in deciphering the role of small molecules in complex environments.[28] A core design element in ABS is a chemical reaction that can generate a unique spectral signal with high selectivity in response to the target analyte (Fig. 1A). Many activity-based sensors have been developed over the years to monitor, for example, reactive nitrogen species (RNS) or oxygen species (ROS).[29,30] ABS approaches have also been developed to detect reactive carbon species (RCS), mainly formaldehyde and carbon monoxide.[31] The high selectivity and sensitivity of this approach have led to considerable advances in our understanding of the role played by small molecules in numerous research areas.[28,32,33]

In light of the relevance of CO$_2$ and the power of ABS approaches to sense small molecules, the development of highly selective and sensitive CO$_2$ activity-based sensors would unlock numerous mul-

tidisciplinary applications. Notably, alternative molecular approaches to sense CO$_2$ have been limited to non-selective chemical reactions, such as the reversible attack of amines or N-heterocyclic carbenes onto CO$_2$ forming carbamates or carboxylates,[26,34,35] thus severely limiting the selectivity and sensitivity of those sensing processes, and, ultimately, their utility. These limitations clearly reflect the challenge of identifying a highly selective chemical reaction targeting carbon dioxide, in the presence of a sea of more reactive functional groups and molecules. This challenge, as well as the fact that CO$_2$ can occur in either pure or dissolved form, could explain why the development of a highly selective and sensitive CO$_2$ activity-based sensor has so far remained elusive.

Here we report the design, synthesis, and evaluation of a family of novel, selective, and tunable fluorescent CO$_2$ activity-based sensors, based on a cascade Aza-Wittig reaction as a CO$_2$-responsive mechanism (Fig. 1B). This is the first report that utilizes an iminophosphorane as a CO$_2$-stimulus-responsive trigger. These sensors are suitable for the selective molecular sensing of CO$_2$ in gas mixtures, as well as in both organic and aqueous solutions. We further demonstrate the multidisciplinary applicability of the sensors by detecting CO$_2$ levels from air (~400 ppm) down to single-digit ppm levels in gas mixtures, sensing CO$_2$ formation in chemical catalysis, real-time monitoring of CO$_2$ evolution arising from enzymatic activity, and visualizing CO$_2$ in living cells.

RESULTS AND DISCUSSION

We reasoned that an ideal mechanism for molecular CO$_2$ detection should be composed of three essential design elements: 1) a reactive site able to rapidly and selectively react with CO$_2$; 2) a locking element to selectively trap the initially generated intermediate in an

irreversible manner; and 3) a bound fluorescent reporter that simultaneously, upon reaction, produces a distinct spectral fingerprint, both in absorbance and fluorescence spectra. To design a molecular sensor which meets these criteria, we turned our attention to iminophosphoranes, which have emerged as mild reactive handles in Staudinger ligation reactions.[36,37] A less appreciated feature of iminophosphoranes is their ability to react with CO_2 under mild conditions, in a process known as the Aza-Wittig reaction, to form a reactive isocyanate.[38,39] We hypothesized that an activity-based sensor for CO_2 could be composed of a reactive aryl iminophosphorane tethered to a fluorogenic molecule with a pendant amine as locking element (Fig. 1C). Our envisioned cascade activation pathway would start with a reaction between CO_2 and the iminophosphorane group to form an isocyanate, which could subsequently react intramolecularly with the suitably placed nucleophilic amine to form a urea moiety.[40,41] In this process, we surmised that the lone pair of the fluorophore's pendant amine, upon conversion to urea, would dramatically change the compound's electronic properties, resulting in a distinct spectral fingerprint.
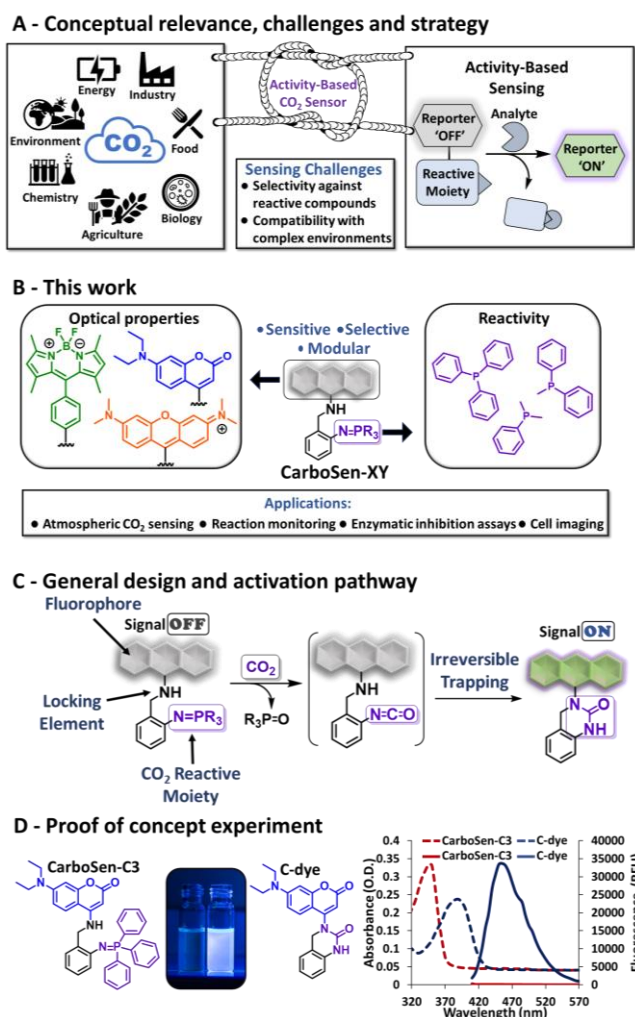

Fig. 1. (A) Conceptual relevance, challenges, and strategy in this study. (B) Scope of this study and nomenclature of the sensors. The "X" refers to the fluorescent motif: C-Coumarin (blue), B-BODIPY (green), R-Rhodamine (orange). The "Y" refers to the number of the iminophosphorane phenyl substituents. (C) General design and activation pathway of the envisioned CO_2 sensors. (D) Chemical structures, absorbance (dashed line), and emission (solid line, Ex = 390 nm) spectra of CarboSen-C3 and C-dye [20 μM] in DMSO. Photo was taken under 380 nm illumination.

We validated our hypothesis experimentally by synthesizing CarboSen-C3 and its corresponding urea product (C-dye) and measuring their spectral properties in DMSO and other solvents (Fig. 1D and S1.1). As predicted, CarboSen-C3 and C-dye exhibit distinct absorbance and emission maxima in all tested solvents. We next evaluated the performance of CarboSen-C3 in the presence and absence of CO_2 (Fig. 2A). Upon bubbling a stream of gaseous CO_2 a strong fluorescence response, which further increased over time, was detected with an emission maximum at 460 nm, identical to the spectrum of C-dye. The turn-on response was saturated at a signal-to-noise ratio of 260. This value demonstrates the high sensitivity of our fluorescence-based sensing approach. Analysis of the reaction using UPLC-MS confirmed the formation of C-dye (Fig. S2). Further controls using an independently synthesized aniline (CarboSen-C-NH2), which is a possible by-product arising from hydrolysis of the iminophosphorane or isocyanate groups, showed that its spectral properties do not interfere with that of C-dye (Fig. S1.1).

The reaction kinetics were next investigated by measuring fluorescence at different time points using varying concentrations of either CarboSen-C3 or CO_2. The reaction shows a first-order dependence on both [CarboSen-C3] and [CO_2] (Fig. S3), pointing towards the initial intermolecular isocyanate formation as the rate-determining step. Next, gas mixtures with different ratios of CO_2/N_2 were bubbled through solutions containing CarboSen-C3 at a constant volume and rate (with a mass flow controller), showing a CO_2 dose-dependent response (Fig. S4). We also found that our sensor is capable of reliably detecting CO_2 in both polar and apolar solvents (Fig. S5). Importantly, activation was observed even in water, boding well for a wide range of applications. Finally, we evaluated the selectivity of CarboSen-C3 against a panel of relevant reactive carbon species (RCS) in the absence of CO_2 (Fig. 2B, RED). Impressively, CarboSen-C3 exhibited only background fluorescence in response to all tested analytes, with the exception of triphosgene, which gave a complex mixture of products. This experiment demonstrates the sensor's exquisite selectivity for CO_2 over other reactive carbon species. Additionally, after 30 minutes, CO_2 was added to all tested RCS samples and the emission was measured again (Fig. 2B, BLUE). The successful activation of the sensor with CO_2 in the presence of several RCS clearly shows that these compounds did not negatively interfere with the fluorescence read-out.

The general design of our CarboSen sensors is composed of a linker connecting two functional moieties: a CO_2-responsive site and a fluorophore. This endows our strategy with high modularity, as adjusting these two moieties can be used to fine-tune the sensor's properties for different applications. In particular, the exchange of the substituents bound to phosphorus (PR3) can provide a useful handle to control the sensor's reactivity towards CO_2. Two new sensors were prepared accordingly, CarboSen-C2 and CarboSen-C1 (Fig. 2C). It was found that the $t_{1/2}$ of the fluorescent response of CarboSen-C3 is ~5 hours while for CarboSen-C2 and CarboSen-C1 the $t_{1/2}$ were ~5 minutes and ~1 minute, respectively, clearly showing the tunability of this system.

The ability to fine-tune the spectral properties of the sensor is also crucial for downstream applications.[42] We thus envisaged extending our strategy to two other widely used fluorophores, BODIPY and rhodamine, generating the new sensors CarboSen-B3 and CarboSen-R3, respectively (Fig. 2D). These fluorophores have found use in many applications and their optical parameters (such as excitation and emission) are suited for most existing instruments such as confocal microscopes and plate readers.[43–46] Moreover, these dyes are often compatible with applications in aqueous media and cell assays. The optical spectra of CarboSen-B3 and CarboSen-R3 were measured, as well as the resulting activated fluorescent products. Similar to the coumarin scaffold, the spectral properties of the

sensors differ significantly from that of their corresponding fluorescent products (Fig. S1.2 and S1.3). Both sensors exhibited negligible fluorescence in the absence of CO_2, however, a strong fluorescence signal was observed upon bubbling a stream of gaseous CO_2 through the solution (Fig. 2D). Like CarboSen-C3, these sensors exhibited a dose-dependent response to altering levels of CO_2. Overall, these results showcase the modularity of the CarboSen family. Not only can the rate of CO_2 detection be controlled by the choice of the iminophosphorane functionality, but the fluorophore can also be swapped or functionalized to adapt to different application requirements. The spectroscopic parameters for selected CarboSen sensors and their corresponding fluorescent products can be seen in Figure S7.
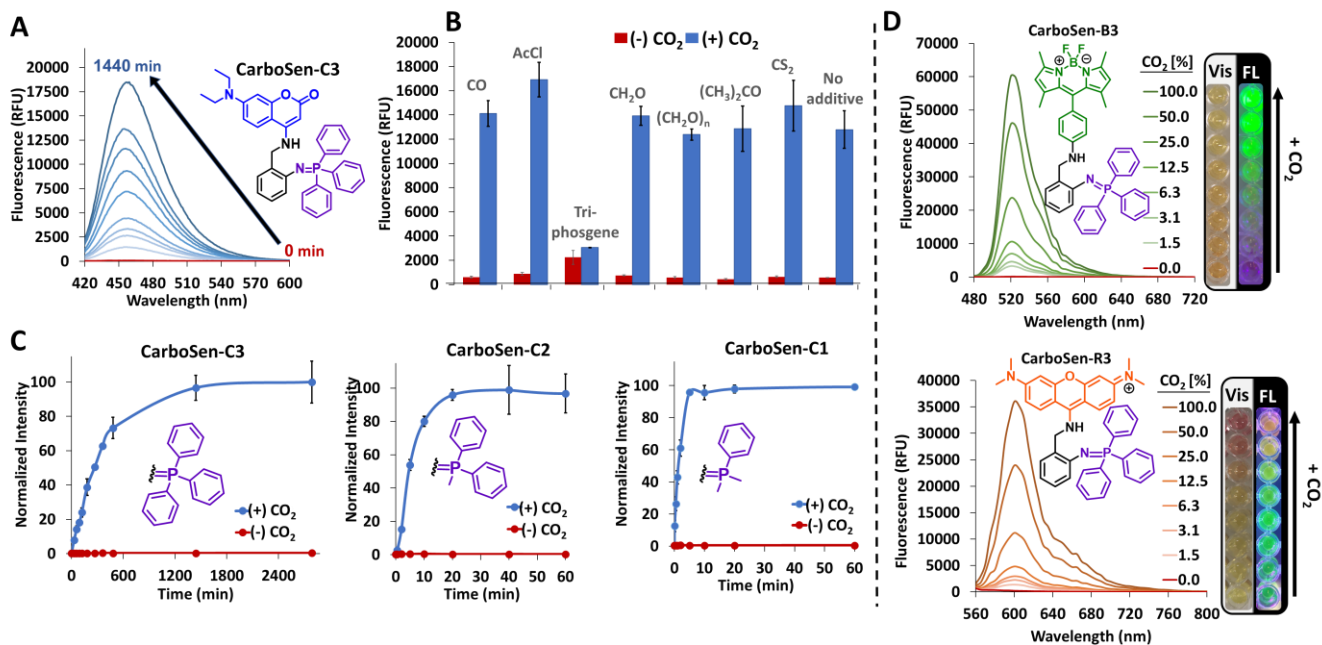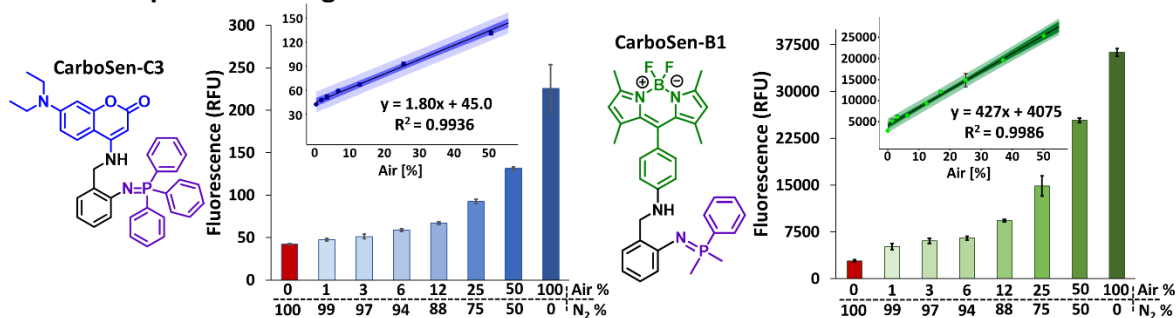

Fig. 2. Structural modularity and activity of the CO_2 ABS approach. (A) Time-resolved fluorescence spectra of CarboSen-C3 [100 µM] in DMSO in the presence and absence of CO_2 [25 mL, 15 s at 100 mL/min]; Ex = 390 nm, Em = 460 nm. (B) Fluorescence response of CarboSen-C3 [100 µM] to reactive carbon species [200 µM] in DMSO (RED). Gaseous CO_2 was bubbled through the solution 30 minutes after the addition of the RCS (BLUE). The gases CO and CO_2 were added using a flow meter [4 mL, 5 s at 50 mL/min]. Ex = 390 nm, Em = 460 nm. (C) Fluorescence kinetic profiles of CarboSen-C3, CarboSen-C2, and CarboSen-C1 [100 µM] in DMSO in the presence and absence of CO_2 [25 mL, 15 s at 100 mL/min]; Ex = 390 nm, Em = 460 nm]. (D) Fluorescence spectral dose-response of CarboSen-B3 and CarboSen-R3 sensors [100 µM] in DMSO to altering ratios of CO_2/N_2 gas mixtures [25 mL, 15 s at 100 mL/min]; CarboSen-B3 Ex = 450 nm, CarboSen-R3 Ex = 530 nm. Photos show the dose-response as seen with the naked eye with (FL) and without (Vis) 380 nm UV flashlight. Measurements were performed in triplicates and error bars denote standard deviation (Mean ± SD; n = 3).

Having uniquely selective and sensitive CO_2 sensors in hand, we next turned our attention to demonstrate the applicability of these compounds through proof-of-concept experiments across a wide range of scientific disciplines (Fig. 3). First, we evaluated the sensors' potential use for sensing atmospheric CO_2 levels (Fig. 3A). Compressed air was used as the CO_2 source and diluted with nitrogen gas. When exposed to different air/N2 mixtures, solutions of CarboSen-C3 and CarboSen-B1 both exhibited a fluorescence dose response and were able to detect atmospheric CO_2 even from a mixture that contains ~2% air (~8 ppm) (Fig. S6). This experiment demonstrates the high sensitivity of our sensors and their potential uses for sensing CO_2 in gas mixtures (Movies M1 and M2).
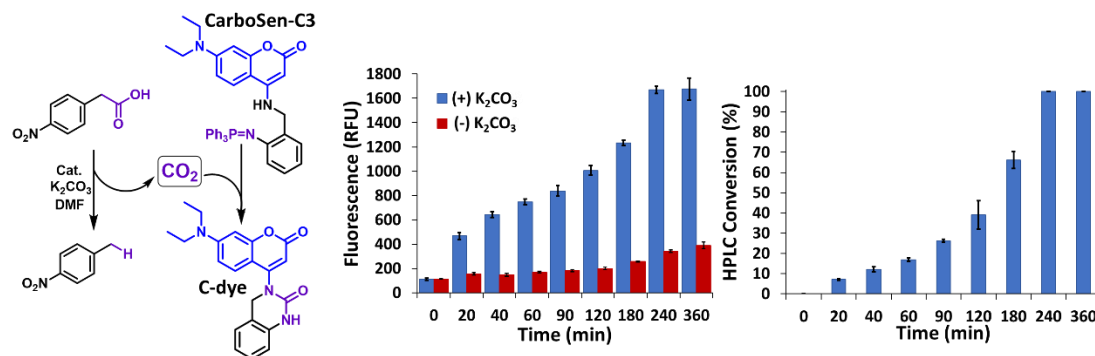
In contrast to monitoring atmospheric CO_2, sensing CO_2 in solution, especially in microscale settings often encountered in biology or chemistry research, can be challenging using state-of-the-art detection methods. An area of chemical catalysis that has recently

seen much interest is the field of catalytic decarboxylative reactions,[47–49] which employs ubiquitous carboxylic acid feedstocks as reagents. As a proof-of-concept to demonstrate the sensors' potential for both the discovery of novel decarboxylation reactions and reaction monitoring, we focused on a model benzylic decarboxylative process.[7] Standard protocols were carried out with only one alteration, namely the addition of CarboSen-C3 [100 µM]. During the course of the reaction, CO_2 is generated and subsequently captured by the sensor, giving rise to a fluorescence signal (Fig. 3B). Therefore, a simple fluorescence measurement can quickly indicate the reaction outcome or progress,[50] bypassing the use of more complex techniques (e.g. GC-MS or IR). A time-dependent experiment showed a correlation between the generated fluorescence signal and the reaction progress, as confirmed by HPLC monitoring. This assay clearly shows the advantage of fluorescence techniques such as their high throughput and simplicity, and demonstrates the sensors' potential for applications in chemical reaction discovery and monitoring.[51,52]

A - Atmospheric sensing

CarboSen-C3

y = 1.80x + 45.0
R² = 0.9936

CarboSen-B1

y = 427x + 4075
R² = 0.9986

| Air % | 0 | 1 | 3 | 6 | 12 | 25 | 50 | 100 |
| N₂ % | 100 | 99 | 97 | 94 | 88 | 75 | 50 | 0 |

B - Monitoring CO₂ evolution in catalytic reaction

CarboSen-C3

$Ph_3P=N$

Cat.
K_2CO_3
DMF

CO_2

C-dye

(+) K_2CO_3
(-) K_2CO_3

C – Monitoring enzymatic activity

CarboSen-R2

Urease

H_2N—C(=O)—NH_2

PBS 7.4

R-dye

Urea concentration

10 mM   5 mM   2.5 mM   1 mM
0.5 mM   0.25 mM   0.1 mM   0 mM

Urease concentration

100 U/mL   50 U/mL   25 U/mL   10 U/mL
5 U/mL   2.5 U/mL   1 U/mL   0 U/mL

(-) Inhibitor

(-) Inhibitor
(-) Urea

0 min   8 min   15 min   30 min   45 min

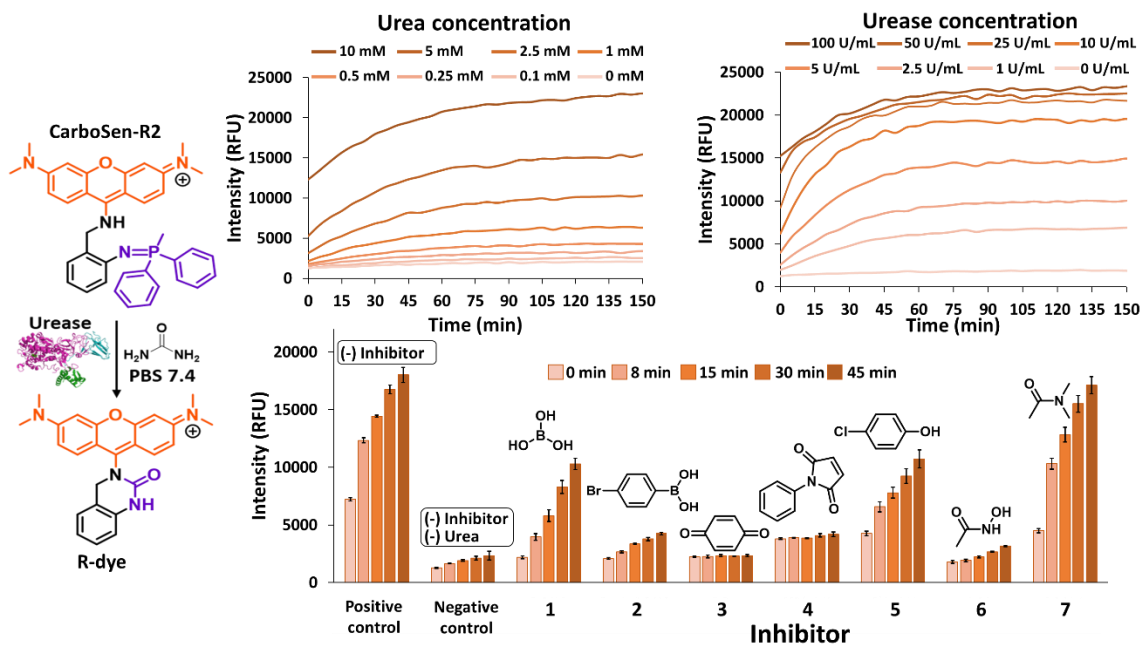Positive control   Negative control   1   2   3   4   5   6   7

Inhibitor

Fig. 3. Model application for CO₂ sensing. (A) Sensing atmospheric gas mixtures – fluorescence spectral dose-response of CarboSen-C3 [100 µM] and CarboSen-B1 [20 µM] in DMSO with altering ratios of air/N₂ gas mixtures [25 mL, 15 s at 100 mL/min]. For CarboSen-C3, Ex = 390 nm, Em = 460 nm. For CarboSen-B1, Ex = 450 nm, Em = 520 nm. (B) Catalytic reaction monitoring – time-resolved fluorescence spectra of CarboSen-C3 [100 µM, Ex = 390 nm, Em = 460 nm] used within the solvent of a model decarboxylative reaction (with and without K₂CO₃, reaction concentration: 0.01 M) and the corresponding HPLC analysis. (C) Enzymatic activity monitoring and model inhibition assay – Fluorescence response of CarboSen-R2 [50 µM, 1% DMSO, Ex = 540 nm, Em = 600 nm]. Top - kinetic profiles in response to altering concentrations of urea and urease (from Canavalia ensiformis, Jack bean, Type IX). Bottom – Model inhibition assay in PBS (pH = 7.4, urease [10 U/mL], urea [1 mM]) using inhibitors 1-6 and control compound 7. Bars represent the mean emission intensity at 0, 8, 15, 30, and 45 minutes. For experimental details see SI. Measurements were performed in triplicates and error bars denote standard deviation (Mean ± SD; n = 3).

We next sought to apply our sensor in a biological context. Tools for fluorescence real-time monitoring of enzymatic activity are widely used to investigate biological processes and signaling pathways in chemical biology.[53,54] Enzymatic activity sensors are important in assay development, which in turn are critical for the identification of ligands and inhibitors of the enzymes themselves.[55] We reasoned that the CarboSen sensors can be applied to such screening assays in monitoring enzymatic reactions that release CO_2. To experimentally support this idea, we focused on urease as a model system. Ureases are nickel-based metalloenzymes that hydrolyze urea to ammonium and CO_2.[56] We subjected CarboSen-R2 (Fig. S7 and Fig. S8) to an enzymatic assay in phosphate buffered saline (PBS) with varying amounts of both urea and urease (Fig. 3C). The sensor was able to distinguish between the production of CO_2 aris-

ing from various urea/urease concentrations. In the absence of either urea or urease only the background response was observed. Next, we conducted a urease inhibition assay. Compounds 1-6 were expected to affect the enzymatic activity in accordance with reported literature,[56] while the control compound 7 should not decrease the enzymatic activity. Compounds 3, 4, and 6 shut down urease activity completely (no CO_2 emission), while on the other hand, compounds 1, 2, and 5 led to low level activity, according to the fluorescence spectra (Fig. 3C). In addition, control compound 7 had a negligible effect on the activity. These results illustrate the applicability of our sensors for relevant enzymatic monitoring assays. In addition, they demonstrate the power of our approach to monitor the formation of minor amounts of CO_2 in solution and in a small, confined space, such as in a well plate.
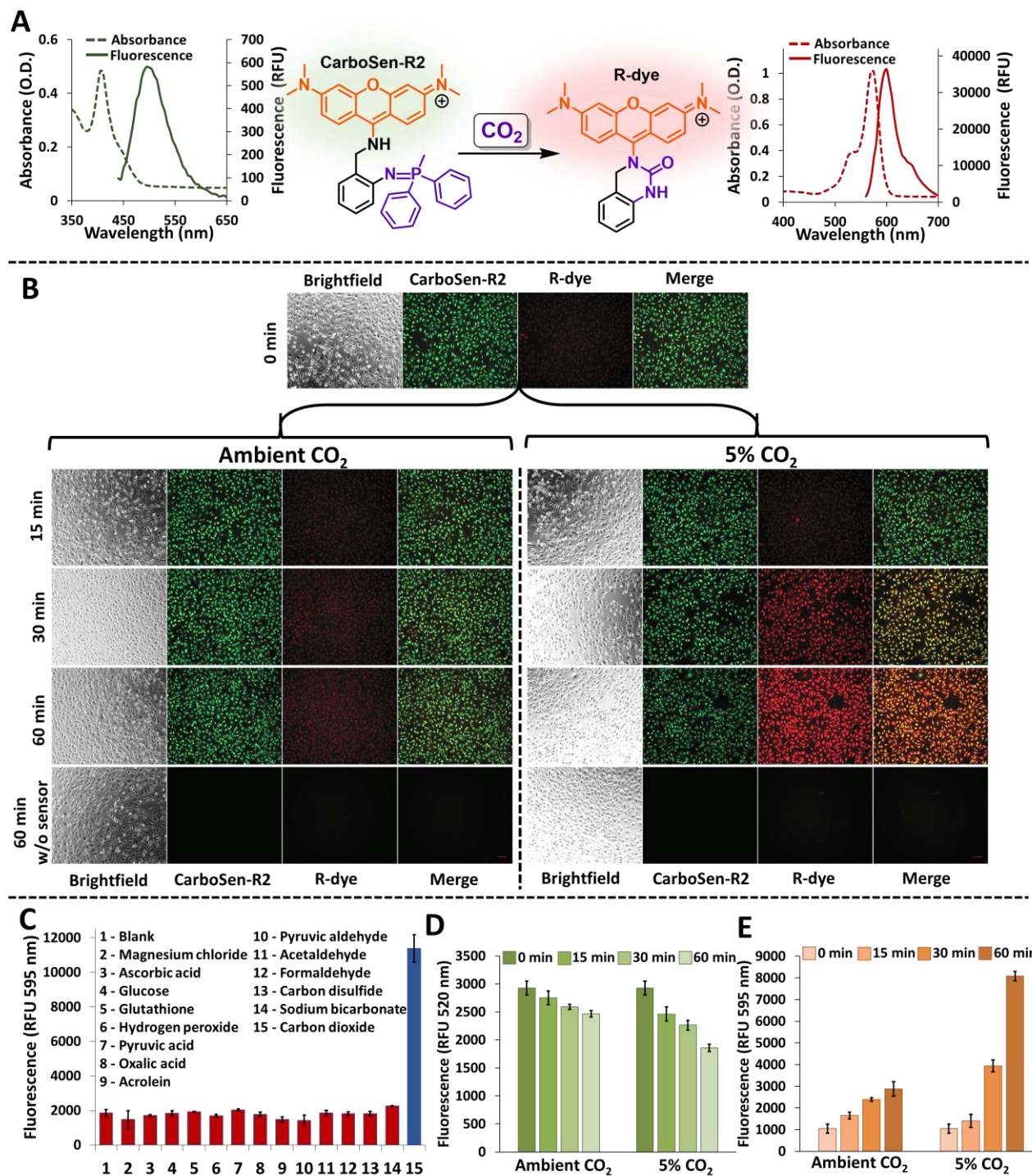
Fig. 4. HeLa cell imaging assay. (A) Spectral properties of CarboSen-R2 and R-Dye [20 µM, 1% DMSO] in PBS (pH = 7.4). (B) Live-cell microscopy images of CarboSen-R2 [5 µM, 0.05% DMSO, 0.05% glycerol] in response to exogenous CO_2 addition in HeLa cells. Cells were treated with CarboSen-R2 for 10 min, at 37 °C in ambient atmospheric CO_2. Subsequently, the cells were washed to remove extracellular sensor, followed by further incubation of the cells either in ambient or 5% CO_2. Images were taken at 0, 15, 30, 60 minutes. (C) Fluorescence response of CarboSen-R2 [50 µM] to common biological analytes [500 µM, 10 eq] in PBS (pH = 7.4). The CO_2 was added using a flow meter [10 mL, 10 s at 60 mL/min] Ex = 540 nm, Em = 595 nm. (D) Quantification of the results in the green fluorescence channel at different time points. Ex = 430 nm, Em = 520 nm. (E) Quantification of the results in the red fluorescence channel at different time points. Ex = 540 nm, Em = 595 nm. The bar plots represent the mean values of four independent triplicate experiments with the respective standard deviations (Mean ± SD; n = 4).

Encouraged by the promising results obtained so far, we finally sought to test our sensors in a cell culture setting. Sensing CO_2 in such a complex environment is an unmet challenge due to the presence of numerous reactive molecules. We focused on CarboSen-R2 as it exhibits a shift in fluorescence from green to red upon reacting with CO_2. This change in emission wavelength offers the opportunity to visualize both CarboSen-R2 and R-dye simultaneously (Fig. 4A). In addition, this sensor displays a selective spectral response towards CO_2 compared to common cellular analytes including carbonate (Fig. 4C and S9). HeLa cells were incubated with CarboSen-R2 [5 µM] for 10 minutes in ambient CO_2 (air, ~0.04%) at 37 °C. The cells were washed thrice to remove the extracellular sensor and imaged (Fig. 4B, t = 0 min). Then, the cells were further incubated under ambient air or at 5% CO_2 and imaged at different time points over 60 min (Fig. 4B). A cell proliferation assay confirmed cells viability during the imaging experiments (Fig. S9). A significant time-dependent fluorescence increase in the red channel and decrease in the green channel was observed under both tested conditions. However, CarboSen-R2's transformation into R-dye occurred visibly faster in the 5% CO_2 atmosphere (Fig. 4D and 4E). Measurements of the fluorescence spectra arising from within the cells were found to exactly match the spectral fingerprint of the activated sensor (Fig. S9), confirming the reaction of CO_2 with the sensor. Importantly, even the cells that were incubated under ambient conditions exhibited a time-dependent response that might be attributed to basal levels of CO_2 production.[57,58] We further observed that the red signal was unevenly distributed throughout the cytoplasm, and mostly excluded from the nucleus (Fig. S10). While this is intriguing, the subcellular localization of the sensor was not within the scope of this study and was not further analyzed. We believe that these results will trigger further studies in living organisms and open up new avenues to improve our understanding of metabolic processes.

In conclusion, we have reported the design, synthesis, and evaluation of a broad family of selective fluorescent CO_2 activity-based sensors. Taking advantage of their unprecedented selectivity, as well as their high modularity, we demonstrated their multidisciplinary applicability in atmospheric sensing, chemical reaction monitoring, enzyme inhibitor screening, and live-cell imaging. These results clearly demonstrate these molecular tools' potential to unleash countless future applications across multiple disciplines that critically rely on the visualization and monitoring of CO_2 at the molecular level.

ASSOCIATED CONTENT

Supporting Information. Experimental Procedures and spectral data. Movies M1 and M2 are also provided. This material is available free of charge via the Internet at http://pubs.acs.org

AUTHOR INFORMATION

Corresponding Author

Bill Morandi − *Laboratorium für Organische Chemie, ETH Zürich, 8093 Zürich, Switzerland;* orcid.org/0000-0003-3968-1424; Email: bill.morandi@org.chem.ethz.ch

Authors

Ori Green − *Laboratorium für Organische Chemie, ETH Zürich, 8093 Zürich, Switzerland;*
Patrick Finkelstein − *Laboratorium für Organische Chemie, ETH Zürich, 8093 Zürich, Switzerland;* orcid.org/0000-0002-5881-3499
Miguel A. Rivero-Crespo− *Laboratorium für Organische Chemie, ETH Zürich, 8093 Zürich, Switzerland*; orcid.org/0000-0003-3968-1424

Marius D. R. Lutz− *Laboratorium für Organische Chemie, ETH Zürich, 8093 Zürich, Switzerland*;
Michael K. Bogdos− *Laboratorium für Organische Chemie, ETH Zürich, 8093 Zürich, Switzerland*;
Michael Burger− *Institute of Pharmaceutical Sciences, ETH Zürich, 8093 Zürich, Switzerland*;
Jean-Christophe Leroux− *Institute of Pharmaceutical Sciences, ETH Zürich, 8093 Zürich, Switzerland*;

REFERENCES

(1)   Clark, M. A.; Domingo, N. G. G.; Colgan, K.; Thakrar, S. K.; Tilman, D.; Lynch, J.; Azevedo, I. L.; Hill, J. D. Global Food System Emissions Could Preclude Achieving the 1.5° and 2°C Climate Change Targets. *Science* **2020**, *370* (6517), 705–708. https://doi.org/10.1126/science.aba7357.

(2)   Field, C. B.; Mach, K. J. Rightsizing Carbon Dioxide Removal. *Science* **2017**, *356* (6339), 706–707. https://doi.org/10.1126/science.aam9726.

(3)   Cummins, E. P.; Strowitzki, M. J.; Taylor, C. T. Mechanisms and Consequences of Oxygen and Carbon Dioxide Sensing in Mammals. *Physiol. Rev.* **2020**, *100* (1), 463–488. https://doi.org/10.1152/physrev.00003.2019.

(4)   Cummins, E. P.; Selfridge, A. C.; Sporn, P. H.; Sznajder, J. I.; Taylor, C. T. Carbon Dioxide-Sensing in Organisms and Its Implications for Human Disease. *Cell. Mol. Life Sci. CMLS* **2014**, *71* (5), 831–845. https://doi.org/10.1007/s00018-013-1470-6.

(5)   Pennisi, E. Carbon Dioxide Increase May Promote 'Insect Apocalypse.' *Science* **2020**, *368* (6490), 459–459. https://doi.org/10.1126/science.368.6490.459.

(6)   Otto, A.; Grube, T.; Schiebahn, S.; Stolten, D. Closing the Loop: Captured CO_2 as a Feedstock in the Chemical Industry. *Energy Environ. Sci.* **2015**, *8* (11), 3283–3297. https://doi.org/10.1039/C5EE02591E.

(7)   Kong, D.; Moon, P. J.; Lui, E. K. J.; Bsharat, O.; Lundgren, R. J. Direct Reversible Decarboxylation from Stable Organic Acids in Dimethylformamide Solution. *Science* **2020**, *369* (6503), 557–561. https://doi.org/10.1126/science.abb4129.

(8)   Liu, Y.; Jessop, P. G.; Cunningham, M.; Eckert, C. A.; Liotta, C. L. Switchable Surfactants. *Science* **2006**, *313* (5789), 958–960. https://doi.org/10.1126/science.1128142.

(9)   Bloom, A. J.; Burger, M.; Asensio, J. S. R.; Cousins, A. B. Carbon Dioxide Enrichment Inhibits Nitrate Assimilation in Wheat and Arabidopsis. *Science* **2010**, *328* (5980), 899–903. https://doi.org/10.1126/science.1186440.

(10) Agrimonti, C.; Lauro, M.; Visioli, G. Smart Agriculture for Food Quality: Facing Climate Change in the 21st Century. *Crit. Rev. Food Sci. Nutr.* **2021**, *61* (6), 971–981. https://doi.org/10.1080/10408398.2020.1749555.

(11) Puligundla, P.; Jung, J.; Ko, S. Carbon Dioxide Sensors for Intelligent Food Packaging Applications. *Food Control* **2012**, *25* (1), 328–333. https://doi.org/10.1016/j.foodcont.2011.10.043.

(12) Shindell, D.; Faluvegi, G.; Seltzer, K.; Shindell, C. Quantified, Localized Health Benefits of Accelerated Carbon Dioxide Emissions Reductions. *Nat. Clim. Change* **2018**, *8* (4), 291–295. https://doi.org/10.1038/s41558-018-0108-y.

(13) El-Betany, A. M. M.; Behiry, E. M.; Gumbleton, M.; Harding, K. G. Humidified Warmed CO_2 Treatment Therapy Strategies Can Save Lives With Mitigation and Suppression of SARS-CoV-2 Infection: An Evidence Review. *Front. Med.* **2020**, *7*, 594295. https://doi.org/10.3389/fmed.2020.594295.

(14) Jha, R. K. Non-Dispersive Infrared Gas Sensing Technology: A Review. *IEEE Sens. J.* **2022**, *22* (1), 6–15. https://doi.org/10.1109/JSEN.2021.3130034.

(15) Hubeau, M.; Thorpe, M. R.; Mincke, J.; Bloemen, J.; Bauweraerts, I.; Minchin, P. E. H.; De Schepper, V.; De Vos, F.; Vanhove, C.; Vandenberghe, S.; Steppe, K. High-Resolution in Vivo Imaging of Xylem-Transported CO_2 in Leaves Based on Real-Time 11C-Tracing. *Front. For. Glob. Change* **2019**, *2*, 25. https://doi.org/10.3389/ffgc.2019.00025.

(16) Severinghaus, J. W.; Bradley, A. F. Electrodes for Blood PO_2 and PCO_2 Determination. *J. Appl. Physiol.* **1958**, *13* (3), 515–520. https://doi.org/10.1152/jappl.1958.13.3.515.

(17) Chandramouli, M.; Boraiah, V.; Shivalingappa, R.; Basavanna, V.; Doddamani, S.; Ningaiah, S. Paper-Based Carbon Dioxide Sensors: Past, Present, and Future Perspectives. *Biointerface Res. Appl. Chem.* **2022**, *12*, 2353–2360. https://doi.org/10.33263/BRIAC122.23532360.

(18) Wang, H.; Vagin, S. I.; Rieger, B.; Meldrum, A. An Ultrasensitive Fluorescent Paper-Based CO_2 Sensor. *ACS Appl. Mater. Interfaces* **2020**, *12* (18), 20507–20513. https://doi.org/10.1021/acsami.0c03405.

(19) Li, X.; Tang, B.; Wu, B.; Hsu, C.; Wang, X. Highly Sensitive Diffraction Grating of Hydrogels as Sensors for Carbon Dioxide Detection. *Ind. Eng. Chem. Res.* **2021**, *60* (12), 4639–4649. https://doi.org/10.1021/acs.iecr.1c00211.

(20) Li, Y.; Young, D. J.; Loh, X. J. Fluorescent Gels: A Review of Synthesis, Properties, Applications and Challenges. *Mater. Chem. Front.* **2019**, *3* (8), 1489–1502. https://doi.org/10.1039/C9QM00127A.

(21) Yoon, B.; Choi, S.-J.; Swager, T. M.; Walsh, G. F. Switchable Single-Walled Carbon Nanotube–Polymer Composites for CO_2 Sensing. *ACS Appl. Mater. Interfaces* **2018**, *10* (39), 33373–33379. https://doi.org/10.1021/acsami.8b11689.

(22) Xu, Q.; Lee, S.; Cho, Y.; Kim, M. H.; Bouffard, J.; Yoon, J. Polydiacetylene-Based Colorimetric and Fluorescent Chemosensor for the Detection of Carbon Dioxide. *J. Am. Chem. Soc.* **2013**, *135* (47), 17751–17754. https://doi.org/10.1021/ja410557x.

(23) Xie, M.-H.; Cai, W.; Chen, X.; Guan, R.-F.; Wang, L.-M.; Hou, G.-H.; Xi, X.-G.; Zhang, Q.-F.; Yang, X.-L.; Shao, R. Novel CO2 Fluorescence Turn-On Quantification Based on a Dynamic AIE-Active Metal–Organic Framework. *ACS Appl. Mater. Interfaces* **2018**, *10* (3), 2868–2873. https://doi.org/10.1021/acsami.7b17793.

(24) Wang, Z.; Ma, H.; Zhai, T.-L.; Cheng, G.; Xu, Q.; Liu, J.-M.; Yang, J.; Zhang, Q.-M.; Zhang, Q.-P.; Zheng, Y.-S.; Tan, B.; Zhang, C. Networked Cages for Enhanced CO_2 Capture and Sensing. *Adv. Sci.* **2018**, *5* (7), 1800141. https://doi.org/10.1002/advs.201800141.

(25) Rezk, M. Y.; Sharma, J.; Gartia, M. R. Nanomaterial-Based CO_2 Sensors. *Nanomaterials* **2020**, *10* (11), 2251. https://doi.org/10.3390/nano10112251.

(26) Zhu, J.; Jia, P.; Li, N.; Tan, S.; Huang, J.; Xu, L. Small-Molecule Fluorescent Probes for the Detection of Carbon Dioxide.

(27) Li, H.-J.; Mellerup, S. K.; Wang, X.; Wang, S. D−π–A Triarylboranes as Reversible Fluorescent Probes for CO_2 and Temperature. *Org. Lett.* **2019**, *21* (8), 2838–2842. https://doi.org/10.1021/acs.orglett.9b00831.

(28) Bruemmer, K. J.; Crossley, S. W. M.; Chang, C. J. Activity-Based Sensing: A Synthetic Methods Approach for Selective Molecular Imaging and Beyond. *Angew. Chem. Int. Ed.* **2020**, *59* (33), 13734–13762. https://doi.org/10.1002/anie.201909690.

(29) Bezner, B. J.; Ryan, L. S.; Lippert, A. R. Reaction-Based Luminescent Probes for Reactive Sulfur, Oxygen, and Nitrogen Species: Analytical Techniques and Recent Progress. *Anal. Chem.* **2020**, *92* (1), 309–326. https://doi.org/10.1021/acs.analchem.9b04990.

(30) Wu, D.; Sedgwick, A. C.; Gunnlaugsson, T.; Akkaya, E. U.; Yoon, J.; James, T. D. Fluorescent Chemosensors: The Past, Present and Future. *Chem. Soc. Rev.* **2017**, *46* (23), 7105–7123. https://doi.org/10.1039/C7CS00240H.

(31) Ohata, J.; Bruemmer, K. J.; Chang, C. J. Activity-Based Sensing Methods for Monitoring the Reactive Carbon Species Carbon Monoxide and Formaldehyde in Living Systems. *Acc. Chem. Res.* **2019**, *52* (10), 2841–2848. https://doi.org/10.1021/acs.accounts.9b00386.

(32) Chu, H.; Yang, L.; Yu, L.; Kim, J.; Zhou, J.; Li, M.; Kim, J. S. Fluorescent Probes in Public Health and Public Safety. *Coord. Chem. Rev.* **2021**, *449*, 214208. https://doi.org/10.1016/j.ccr.2021.214208.

(33) Duan, N.; Wang, H.; Li, Y.; Yang, S.; Tian, H.; Sun, B. The Research Progress of Organic Fluorescent Probe Applied in Food and Drinking Water Detection. *Coord. Chem. Rev.* **2021**, *427*, 213557. https://doi.org/10.1016/j.ccr.2020.213557.

(34) Liu, Y.; Tang, Y.; Barashkov, N. N.; Irgibaeva, I. S.; Lam, J. W. Y.; Hu, R.; Birimzhanova, D.; Yu, Y.; Tang, B. Z. Fluorescent Chemosensor for Detection and Quantitation of Carbon Dioxide Gas. *J. Am. Chem. Soc.* **2010**, *132* (40), 13951–13953. https://doi.org/10.1021/ja103947j.

(35) Guo, Z.; Song, N. R.; Moon, J. H.; Kim, M.; Jun, E. J.; Choi, J.; Lee, J. Y.; Bielawski, C. W.; Sessler, J. L.; Yoon, J. A Benzobisimidazolium-Based Fluorescent and Colorimetric Chemosensor for CO_2. *J. Am. Chem. Soc.* **2012**, *134* (43), 17846–17849. https://doi.org/10.1021/ja306891c.

(36) Schilling, C. I.; Jung, N.; Biskup, M.; Schepers, U.; Bräse, S. Bioconjugation Viaazide–Staudinger Ligation: An Overview. *Chem. Soc. Rev.* **2011**, *40* (9), 4840–4871. https://doi.org/10.1039/C0CS00123F.

(37) Saxon, E.; Bertozzi, C. R. Cell Surface Engineering by a Modified Staudinger Reaction. *Science* **2000**, *287* (5460), 2007–2010. https://doi.org/10.1126/science.287.5460.2007.

(38) Adda, A.; Sediki, H. Theoretical Study of the Aza-Wittig Reaction, $Me_3P=NR$ (R = Methyl or Phenyl) with Aldehyde Using the DFT and DFT-D Methods (Dispersion Correction). *Chem. Proc.* **2020**, *3* (1), 47. https://doi.org/10.3390/ecsoc-24-08349.

(39) Staudinger, H.; Meyer, J. Über Neue Organische Phosphorverbindungen III. Phosphinmethylenderivate Und Phosphinimine. *Helv. Chim. Acta* **1919**, *2* (1), 635–646. https://doi.org/10.1002/hlca.19190020164.

(40) Kovács, J.; Pintér, I.; Messmer, A.; Tóth, G.; Duddeck, H. A New Route to Cyclic Urea Derivatives of Sugars via Phosphinimines. *Carbohydr. Res.* **1987**, *166* (1), 101–111. https://doi.org/10.1016/0008-6215(87)80047-2.

(41) Del Vecchio, A.; Caillé, F.; Chevalier, A.; Loreau, O.; Horkka, K.; Halldin, C.; Schou, M.; Camus, N.; Kessler, P.; Kuhnast, B.; Taran, F.; Audisio, D. Late-Stage Isotopic Carbon Labeling of Pharmaceutically Relevant Cyclic Ureas Directly from CO_2. *Angew. Chem. Int. Ed.* **2018**, *57* (31), 9744–9748. https://doi.org/10.1002/anie.201804838.

Chin. Chem. Lett. **2018**, *29* (10), 1445–1450. https://doi.org/10.1016/j.cclet.2018.09.002.

(42) Grimm, J. B.; Muthusamy, A. K.; Liang, Y.; Brown, T. A.; Lemon, W. C.; Patel, R.; Lu, R.; Macklin, J. J.; Keller, P. J.; Ji, N.; Lavis, L. D. A General Method to Fine-Tune Fluorophores for Live-Cell and in Vivo Imaging. *Nat. Methods* **2017**, *14* (10), 987–994. https://doi.org/10.1038/nmeth.4403.

(43) Beija, M.; Afonso, C. A. M.; Martinho, J. M. G. Synthesis and Applications of Rhodamine Derivatives as Fluorescent Probes. *Chem. Soc. Rev.* **2009**, *38* (8), 2410–2433. https://doi.org/10.1039/B901612K.

(44) Jia, S.; Ramos-Torres, K. M.; Kolemen, S.; Ackerman, C. M.; Chang, C. J. Tuning the Color Palette of Fluorescent Copper Sensors through Systematic Heteroatom Substitution at Rhodol Cores. *ACS Chem. Biol.* **2018**, *13* (7), 1844–1852. https://doi.org/10.1021/acschembio.7b00748.

(45) Ulrich, G.; Ziessel, R.; Harriman, A. The Chemistry of Fluorescent Bodipy Dyes: Versatility Unsurpassed. *Angew. Chem. Int. Ed.* **2008**, *47* (7), 1184–1201. https://doi.org/10.1002/anie.200702070.

(46) Fan, G.; Yang, L.; Chen, Z. Water-Soluble BODIPY and Aza-BODIPY Dyes: Synthetic Progress and Applications. *Front. Chem. Sci. Eng.* **2014**, *8* (4), 405–417. https://doi.org/10.1007/s11705-014-1445-7.

(47) Li, C.; Wang, J.; Barton, L. M.; Yu, S.; Tian, M.; Peters, D. S.; Kumar, M.; Yu, A. W.; Johnson, K. A.; Chatterjee, A. K.; Yan, M.; Baran, P. S. Decarboxylative Borylation. *Science* **2017**, *356* (6342), eaam7355. https://doi.org/10.1126/science.aam7355.

(48) Rodríguez, N.; Goossen, L. J. Decarboxylative Coupling Reactions: A Modern Strategy for C–C-Bond Formation. *Chem. Soc. Rev.* **2011**, *40* (10), 5030–5048. https://doi.org/10.1039/C1CS15093F.

(49) Zuo, Z.; Ahneman, D. T.; Chu, L.; Terrett, J. A.; Doyle, A. G.; MacMillan, D. W. C. Merging Photoredox with Nickel Catalysis: Coupling of α-Carboxyl Sp3-Carbons with Aryl Halides. *Science* **2014**, *345* (6195), 437–440. https://doi.org/10.1126/science.1255525.

(50) Collins, K. D.; Gensch, T.; Glorius, F. Contemporary Screening Approaches to Reaction Discovery and Development. *Nat. Chem.* **2014**, *6* (10), 859–871. https://doi.org/10.1038/nchem.2062.

(51) Fang, X.; Zheng, Y.; Duan, Y.; Liu, Y.; Zhong, W. Recent Advances in Design of Fluorescence-Based Assays for High-Throughput Screening. *Anal. Chem.* **2019**, *91* (1), 482–504. https://doi.org/10.1021/acs.analchem.8b05303.

(52) Inglese, J.; Johnson, R. L.; Simeonov, A.; Xia, M.; Zheng, W.; Austin, C. P.; Auld, D. S. High-Throughput Screening Assays for the Identification of Chemical Probes. *Nat. Chem. Biol.* **2007**, *3* (8), 466–479. https://doi.org/10.1038/nchembio.2007.17.

(53) Liu, H.-W.; Chen, L.; Xu, C.; Li, Z.; Zhang, H.; Zhang, X.-B.; Tan, W. Recent Progresses in Small-Molecule Enzymatic Fluorescent Probes for Cancer Imaging. *Chem. Soc. Rev.* **2018**, *47* (18), 7140–7180. https://doi.org/10.1039/C7CS00862G.

(54) Sanchez, M. I.; de Vries, L. E.; Lehmann, C.; Lee, J. T.; Ang, K. K.; Wilson, C.; Chen, S.; Arkin, M. R.; Bogyo, M.; Deu, E. Identification of Plasmodium Dipeptidyl Aminopeptidase Allosteric Inhibitors by High Throughput Screening. *PloS One* **2019**, *14* (12), e0226270. https://doi.org/10.1371/journal.pone.0226270.

(55) Zielonka, J.; Zielonka, M.; Cheng, G.; Hardy, M.; Kalyanaraman, B. High-Throughput Screening of NOX Inhibitors. In *NADPH Oxidases: Methods and Protocols*; Knaus, U. G., Leto, T. L., Eds.; Methods in Molecular Biology; Springer: New York, NY, 2019; pp 429–446. https://doi.org/10.1007/978-1-4939-9424-3_25.

(56) Svane, S.; Sigurdarson, J. J.; Finkenwirth, F.; Eitinger, T.; Karring, H. Inhibition of Urease Activity by Different Compounds Provides Insight into the Modulation and Association of Bacterial Nickel Import and Ureolysis. *Sci. Rep.* **2020**, *10* (1), 8503. https://doi.org/10.1038/s41598-020-65107-9.

(57) Chen, D.; Wang, H.; Dong, L.; Liu, P.; Zhang, Y.; Shi, J.; Feng, X.; Zhi, J.; Tong, B.; Dong, Y. The Fluorescent Bioprobe with Aggregation-Induced Emission Features for Monitoring to Carbon Dioxide Generation Rate in Single Living Cell and Early Identification of Cancer Cells. *Biomaterials* **2016**, *103*, 67–74. https://doi.org/10.1016/j.biomaterials.2016.06.055.

(58) Mishra, R. K.; Vijayakumar, S.; Mal, A.; Karunakaran, V.; Janardhanan, J. C.; Maiti, K. K.; Praveen, V. K.; Ajayaghosh, A. Bimodal Detection of Carbon Dioxide Using Fluorescent Molecular Aggregates. *Chem. Commun.* **2019**, *55* (43), 6046–6049. https://doi.org/10.1039/C9CC01564G.

Insert Table of Contents artwork here